

Emulation of a Hydrokinetic Turbine to Assess Control and Grid Integration

Robert J. Cavagnaro*, Brian Polagye*, Jim Thomson*, Brian Fabien*, Dominic Forbush*, Levi Kilcher†, James Donegan‡, Jarlath McEntee‡

*NNMREC, University of Washington, Seattle, WA 98195, USA

rcav@uw.edu, bpolagye@uw.edu, jthomson@apl.washington.edu, fabien@uw.edu, forbudom@uw.edu

†National Renewable Energy Laboratory, Golden, CO 80401, USA

levi.kilcher@nrel.gov

‡Ocean Renewable Power Company, Portland, ME 04101, USA

jdonegan@orpc.co, jmcentee@orpc.co

Abstract—A horizontally-oriented cross-flow turbine is dynamically emulated on hardware to investigate control strategies and grid integration. A representative inflow time-series with a mean of 2 m/s is generated from high-resolution flow measurements of a riverine site and is used to drive emulation. Power output during emulation under similar input and loading conditions yields agreement with field measurements to within 3% at high power, near-optimal levels. Constant tip-speed ratio and constant speed proportional plus integral control schemes are compared to optimal nonlinear control and constant resistance regulation. All controllers yield similar results in terms of overall system efficiency. The emulated turbine exhibits a stronger reaction to turbulent inflow than the field turbine. The turbine has a lower inertia than the demand of an isolated grid, indicating a secondary source of power with a similar frequency response is necessary if a single turbine cannot meet the entire demand.

Index Terms—Hydrokinetic turbine, riverine, emulation, grid integration, turbine control

I. INTRODUCTION

Energy recovery from hydrokinetic sources may be an attractive option for remote communities adjacent to an appropriate resource. These communities often have weak electrical grids and lack advanced distribution capabilities [1]. Consequently, prior to installation, it is beneficial to understand how a hydrokinetic energy conversion system will perform and the effects of integrating it into existing grid infrastructure. Ocean Renewable Power Company (ORPC) is currently developing a horizontally-oriented helical cross-flow hydrokinetic turbine for use in riverine systems. The RivGen turbine (Fig. 1) is rated to produce 17 kW of electrical power in mean currents of 2.3 m/s. ORPC is characterizing the performance of the turbine in the Kvichak River near Igiugig, Alaska (Fig. 2) a site representative of a hydrokinetic resource suitable for electricity generation in terms of kinetic power density and isolated electricity demand.

Detailed knowledge of incident hydrokinetic current is necessary to accurately determine the efficiency of a turbine system [2]. Therefore, flow characterization measurements are made concurrent to turbine operation in the Kvichak River. Acoustic Doppler sensing techniques are used to measure variation in mean flow speed, turbulence content, and lateral

(across-rotor) shear. This characterization, in addition to allowing a performance curve to be developed, can inform a statistical model of the flow that serves as a representative velocity time-series for simulation and emulation models of the turbine-river system.

As power take-off (PTO) components such as a gearbox and generator strongly influence the behavior of a turbine system, it is beneficial to evaluate the performance of the turbine with a PTO [4]. Electromechanical emulation machines (EEMs) are hardware-in-the-loop systems capable of emulating the dynamics of rotating bodies in response to realistic input, include a full, controllable PTO, and are commonly used to evaluate wind energy systems [3]. Previous studies have extended the use of emulators to hydrokinetic turbines to evaluate control strategies, comparing results of emulation to dynamic simulation based on turbine properties [5]–[7]. Additionally, an emulator has successfully matched the performance of a prototype turbine in a laboratory test scenario [8]. However, these studies have not compared results from the emulation technique to those of an actual field-deployed hydrokinetic turbine subject to realistic resource input.

The Conn EEM at MaREI-Beaufort in Cork, Ireland consists of a controllable motor, programmed to emulate the characteristics of a turbine, coupled to a generator. The generator is connected to back-to-back power converters enabling controllable variable-speed operation and integration with the local grid [9]. This machine is herein configured to emulate the dynamics of the RivGen turbine based on performance and resource characterization determined by field trials. Electrical power produced during constant resistive loading in the field is compared to that produced on the EEM under equivalent loads to validate the efficacy of emulation. Once verified, three control schemes intended to minimize the levelized cost of energy are implemented on the EEM to evaluate their performance. Additionally, a typical demand profile for the community of Igiugig is compared to the emulated turbine output to determine possible effects of turbine control strategies on the local grid. The turbine and EEM are briefly described in Section II, in addition to a description of the methods of resource modeling and turbine emulation. Emulation results



Fig. 1. RivGen turbine generator unit prior to deployment in Kvichak River near Igiugig, Alaska



Fig. 2. Kvichak River near Igiugig, Alaska with turbine site and coordinate system denoted

are presented in Section III and discussed in Section IV before conclusions are stated in Section V.

II. METHODS

A. Turbine Description

ORPC's RivGen turbine consists of two 1.4 m diameter rotors of 4.1 m length bracketing a central generator. The 11.5 m² cross-sectional area (A) is centered approximately 3 m above the riverbed. The direct-drive permanent magnet generator output was rectified, transmitted to shore, and dissipated through a load bank of variable resistance (R) for field performance characterization ahead of grid integration. Electrical power (P_E) across the load was measured using a Shark 200 power meter on the DC input to the shore station. Expected P_E is related to R by the generator's voltage constant (K_v) of 513.6 V/rad/s and rotation rate (ω) inferred from voltage measurements as,

$$P_E = \frac{\omega^2 K_v^2}{R}. \quad (1)$$

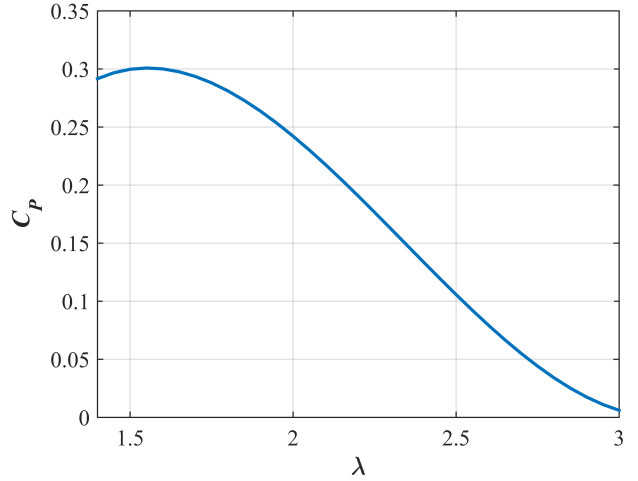


Fig. 3. Estimated performance curve of the RivGen turbine as implemented in emulation assuming a 90% η_E

The total system efficiency (η_S) is the fraction of incident kinetic power converted to electrical power,

$$\eta_S = \frac{P_E}{\frac{1}{2}\rho A U_\infty^3} \quad (2)$$

where ρ is the density of water and U_∞ is the reference inflow velocity. The turbine's mechanical conversion efficiency, or coefficient of performance (C_P) was estimated from field measurements of (2) with an assumption of the electrical efficiency of the generator and power conversion components (η_E) of 0.9 (based on generator characterization) such that,

$$C_P = \frac{\eta_S}{\eta_E}. \quad (3)$$

In [2], η_S was parameterized as a function of the turbine's tip-speed ratio (λ),

$$\lambda = \frac{\omega r}{U_\infty} \quad (4)$$

where r is the rotor radius. Applying the correction for estimated drive train efficiency yields a characteristic curve for the turbine that is a function of C_P and λ (Fig. 3).

B. Resource Characterization Modeling

Flow of the Kvichak River 60 m upstream of the turbine site was measured at high temporal resolution using an acoustic Doppler velocimeter (ADV) attached to a sounding weight and manually deployed from a skiff. Motion of the ADV was synchronously recorded by an inertial motion unit and removed from the velocity measurement [10]. This measurement was used to specify input parameters for the National Renewable Energy Laboratory's PyTurbSim code. PyTurbSim is a turbulence simulation tool specifically tailored for generating resource time-series as input for hydrokinetic device simulation [11]. The software utilizes four statistical measurements of inflow: the mean velocity profile, turbulent kinetic energy (TKE) spectrum, Reynold's stress profile, and

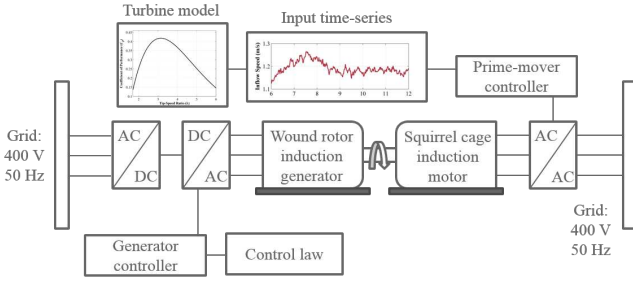


Fig. 4. Schematic of Conn emulator layout

spatial coherence [11]. TKE from the field ADV measurements was determined and matched in the software output time-series. A mean velocity of 2.0 m/s, representative of average inflow velocity across the turbine rotor [2], was specified for the output over a spatial grid 10 m wide by 5 m deep. A logarithmic mean water velocity profile was specified with a uniform Reynold's stress over the spatial domain while the NWTC 'non-IEC' coherence model was used. A high degree of spatial variability in mean flow in the lateral direction observed in the field was not, however, captured [2]. A temporally representative time-series was generated for 300 s (0.0625 s time-step) of 'stationary' inflow. The grid location chosen for this time series was at turbine hub-height in the center of the channel.

C. Conn EEM and Emulation Technique

The 'prime-mover' of the Conn EEM (Fig. 4) used to emulate the turbine is a programmable variable speed squirrel-cage induction motor rated for 20 kW. The motor drive can realize commands of current (converted to torque through calibration) or rotation rate with an internal proportional plus integral (PI) loop. These commands are sent to the drive from a programmable logic controller (PLC) executing a program emulating the RivGen turbine rotor mechanical power output. This program solves for ω numerically from an implementation of a first-order dynamic model of angular acceleration,

$$\dot{\omega} = \frac{1}{J}(\tau_H - \tau_C - B\omega) \quad (5)$$

in which J is the effective turbine and PTO rotational moment of inertia, τ_H is the turbine's hydrodynamic torque, τ_C is the oppositional (control) torque associated with loading from the generator, and B is a damping coefficient representing parasitic frictional losses in the system. Values of J and B are estimated for the turbine as 246 kg-m² and 10 Nm-s/rad respectively. A value of τ_H is determined at each emulation time step based on the current value of the representative U_∞ at the turbine hub-height generated with PyTurbSim, and a value of $C_P(\lambda)$ corresponding to the emulated λ .

Though the prime-mover motor of the EEM is rated for a higher average power than the RivGen turbine system, transient instances from turbulent spikes in emulated velocity up to 2.7 m/s resulted in instantaneous power over 30 kW. These transients manifested in current spikes of 75 A, above

acceptable limits for the motor drive and system wiring. This required emulating the turbine at a lower power level. Therefore, the turbine PTO output was scaled utilizing a method to preserve the system time constant (J/B) by a factor (γ) of 0.5. This scaling is achieved by multiplying the terms in the numerator and denominator of the right-hand side of (5) by γ , ultimately resulting in the emulation of a turbine with a reduced cross sectional area (and hence, power output) by a factor of γ [12]. Additionally, a virtual 20:1 gearbox (gearing ratio N_V) was applied during emulation to align the low-speed, direct drive performance of the actual turbine with the high-speed characteristics of the EEM motor and generator. Utilizing this correction, commanded prime-mover speed (ω_M) during emulation became,

$$\omega_M = N_V \omega. \quad (6)$$

The PTO of the Conn EEM, as implemented for the testing herein, consisted of a wound rotor induction generator rated for 22 kW with its rotor windings shorted to function as a squirrel-cage induction generator. The generator's stator was connected to a series of programmable variable speed drives, the first regulating generator torque (τ_G), and the second maintaining output power at grid bus voltage and frequency. A PLC program was used to specify loading through the regulation of τ_G , which was similarly virtually geared and scaled as,

$$\tau_G = \frac{\gamma}{N_V} \tau_C \quad (7)$$

and relied on a calibration converting commanded torque to generator current demand. As with the prime-mover motor drive, an internal PI loop regulated generator current.

Available measurements from the EEM testing included ω_M from an encoder, τ_G from a rotary torque sensor, generator RMS phase-phase voltage and phase current, and real & reactive power delivered to or supplied from the grid as reported by the grid-side variable speed drive. These parameters were recorded at 50 Hz.

Generator dynamic performance was evaluated by comparing the power output of the field turbine (sampled at 1 Hz) and emulated turbine output (sampled at 50 Hz) in the frequency domain. Actual turbine output under a 6.4 Ω measured resistive load was scaled by γ to match the power level of the emulator under the same load. Linear trends were subtracted from both time-series, which were split into 64 s windows before processing with a fast Fourier transform. The windowed spectra were averaged to create single power spectral density (PSD) series for each signal. Total variance in output was computed as the integral of PSD over the frequency band analyzed.

D. Generator Control Schemes

Four schemes for determining τ_G were implemented to validate the emulation technique against results from field testing, and to evaluate the resulting C_P and η_S over a 300 s turbulent input flow. Validation testing was conducted by

emulating P_E as if the EEM generator was connected to purely resistive load as in (1). Utilizing (6) and (7), the resulting torque commanded was,

$$\tau_G = \frac{\gamma}{N_V \eta_E} \frac{\omega K_v^2}{R} \quad (8)$$

in which the value of R matched field testing measured resistances of 12.5 Ω , 10.4 Ω , 8.8 Ω , 7.6 Ω , 6.4 Ω , and 5.2 Ω . Successful emulation was achieved if output power delivered to the grid under the same load and similar inflow conditions matched power produced by the turbine in field, scaled by γ . Power factor during emulation was maintained at 1.0 to match the purely resistive loads present during field testing.

Two PI controllers were implemented in emulation to maintain a constant, optimal value of λ^* and a constant ω^* equal to the optimal ω corresponding to the mean flow speed of the 300 s input time-series, respectively. Controller action was conducted at a 10 Hz update rate, and proportional (K_P) and integral (K_I) gains were tuned empirically to achieve a balance between tight tracking of λ^* or ω^* and overshooting. The rotation rate PI controller was formulated such that,

$$\tau_G = K_P(\omega - \omega^*) + K_I \int_0^t (\omega - \omega^*) d\tau \quad (9)$$

where t is the total time of the controller action, and τ is the length of a single time step. The integral term was computed numerically in the controller PLC program. The tip-speed ratio PI controller was implemented similarly.

Furthermore, a nonlinear controller specifying an optimal torque command was implemented. This maximum power-point tracking controller (MPPT) specified a control torque based on the square of ω and a gain (K) based on the turbine's parameters and optimal operating point. In emulation, this resulted in a torque command of,

$$\tau_G = K\omega^2 = \frac{\gamma}{N_V} \left(\frac{1}{2} \rho A r^3 \frac{C_{P,max}}{\lambda^{*3}} \right) \omega^2 \quad (10)$$

where λ^* is the tip-speed ratio corresponding to the turbine's maximum C_P .

E. Isolated Grid Demand

Active and reactive power demand and average grid frequency were recorded for the community of Igiugig to investigate its grid dynamics. Demand in kVA, power factor, and average frequency in Hz were measured at a 1 Hz sampling rate for the duration of the RivGen turbine deployment. This data was monitored on ORPC's SCADA system, and was logged in a database. The grid consisted of two diesel generators rated at 50 kVA. Trends in the frequency domain of the load were compared to the field and emulated generators by normalizing the load and power outputs by their respective means and utilizing the same methods as Section II. *C* Active power demand was only considered for this analysis.

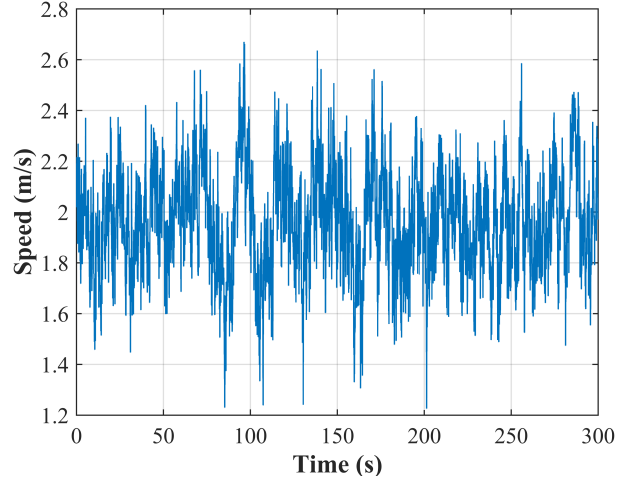


Fig. 5. Water velocity input time series used for emulation

III. RESULTS

A. Velocity Time Series

A single velocity time series (Fig. 5) generated with PyTurbSim from statistical measurements of turbulence made during field trials was used as the input for subsequent emulation (mean velocity of 2.0 m/s). The turbulence intensity is 10.7% and the time series contains a maximum speed of 2.67 m/s and a minimum speed of 1.23 m/s (11 s apart in the time-series).

B. Comparison of Field and Emulated Performance - Constant Resistive Loading

Active power output during field testing of the RivGen turbine under steady, purely resistive loads was measured for 120 s and averaged. P_E scaled by γ is compared to the real power generated under equivalent loading according to (8) during emulation (Fig. 6). Agreement between scaled field and emulated power ranged from 3% difference at the highest power test to 15% at a lower power. Difference in results is attributed to electrical losses relative to output power which are expected to be higher for lower power tests, as these represent a small fraction of the EEM hardware's rated power of 22 kW. Subsequent controller implementations maintain power output near the higher end of the range, where the emulation matches field results. Additionally, some difference may be ascribed to uncertainty in the measurement of the actual turbine load resistance.

C. Emulated Controller Performance

Constant λ , constant ω , and $K\omega^2$ controllers were implemented in emulation to regulate the turbine in response to time-varying inflow conditions. Each controller's effect on emulated turbine ω (from (6)) is shown in Fig. 7. Both constant λ and $K\omega^2$ are variable speed controllers attempting to track the optimal performance point of the turbine, and thus regulate speed to the same setpoint. The constant λ controller, however, overshoots and undershoots the optimal point, a symptom of

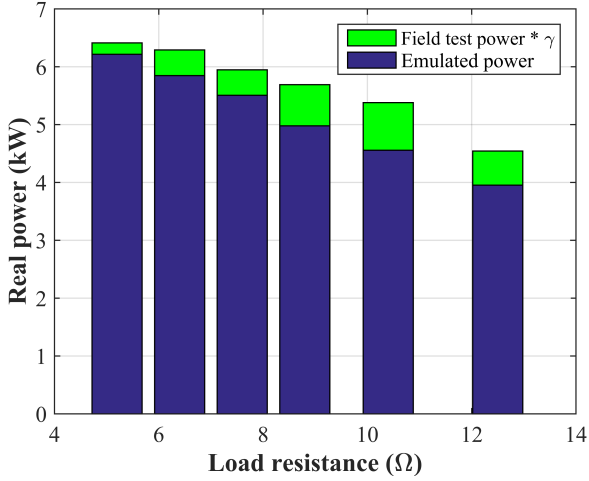


Fig. 6. Resistive loading field and emulation comparison

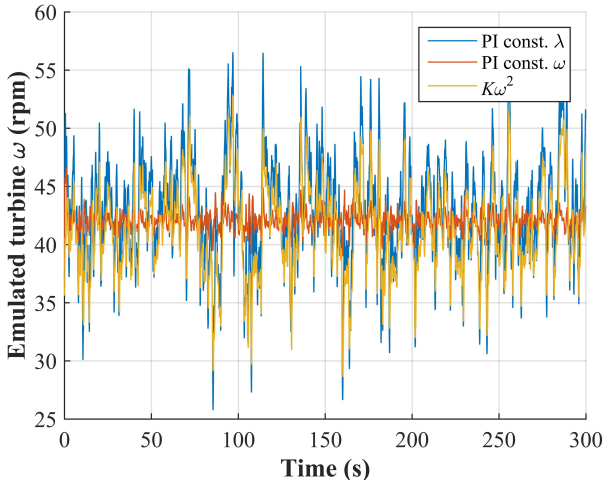


Fig. 7. Emulated turbine speed under control action

linear control. Constant ω control action is clearly seen, as the emulated turbine remains close to the same rotation rate ± 2.5 rpm.

Mean emulated turbine C_P as computed by the PLC-based prime-mover control program was slightly higher for the $K\omega^2$ controller at 0.298, followed by the constant λ and constant ω controllers at 0.295 and 0.293. Hence, there was no significant difference in emulated mechanical efficiency over the 300 s tests. Instantaneous C_P (Fig. 8) dropped momentarily for the constant ω controller during times when the flow speed differed substantially from the mean, corresponding to low frequency, large turbulent fluctuations. Real power delivered to the grid (Fig. 9) exhibited a high degree of similarity for the three controllers. This resulted in nearly identical η_S for each case, with the $K\omega^2$ controller resulting in a mean efficiency of 0.287, and the constant λ and constant ω at 0.280 and 0.284 respectively. The higher system efficiency of the constant ω controller is attributed to the EEM's generator operating at

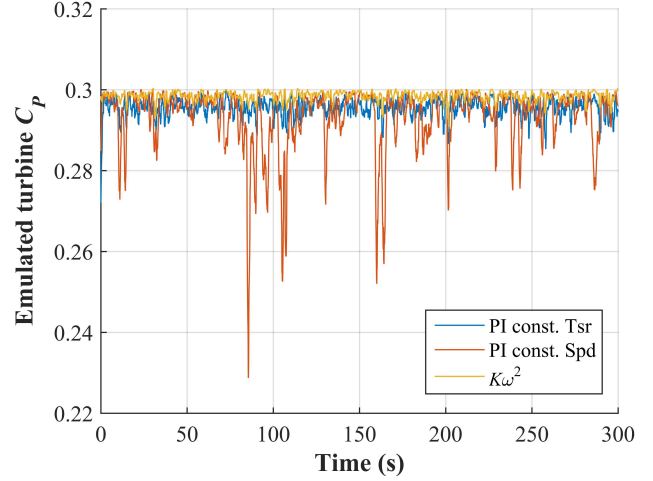


Fig. 8. Instantaneous emulated C_P with 1 s moving average smoothing

a slightly higher electrical efficiency under constant speed operation. Instantaneous values of η_S (Fig. 10) exceeded the maximum C_P of the turbine (0.30). This is thought to be due to a combination of measurement noise, imperfect calibration between commanded τ_G and realized generator current, and imperfect tracking of ω_M during emulation.

Peak PTO torque for the emulation tests under the three controllers varied from 135 Nm for the $K\omega^2$ scheme to 143 Nm and 150 Nm for the PI λ and ω schemes with standard deviations of 15 Nm, 20 Nm, and 22 Nm, respectively. This result indicates the nonlinear controller loads the PTO to a lesser degree by making fewer severe corrections to maintain a setpoint. Conversely, the constant ω controller must make the most severe corrections to maintain constant speed in response to large changes in inflow velocity.

Active controller performance is compared to 'passive' control performance with emulated constant resistive load from (8). Under a loading equivalent to 5.2 Ω , mean turbine C_P was 0.295 with a mean η_S of 0.279. Performance was therefore nearly identical to the active controllers over the 300 s test. PTO loading with this control scheme was less severe, with a peak torque of 104 Nm and standard deviation of 10 Nm. This result is expected, as no corrective action is taken to maintain a setpoint.

D. Comparison of Field and Emulated Dynamic Performance

Power spectra for scaled, field turbine power and emulated power under similar loading conditions are plotted on the same axes (Fig. 11). Though exhibiting a similar trend, emulated turbine output was more variable than field turbine output. Total variance for the turbine was 0.18 kW^2 compared to 1.9 kW^2 for the emulated output. This is thought to be caused by the physical turbine reacting only to turbulent length scales on the order of magnitude of its dimensions (an engulfing gust), and being insensitive to higher frequency turbulence. The turbine's largest dimension is its span-wise length (8.2 m), over which the turbulence and mean flow were substantially

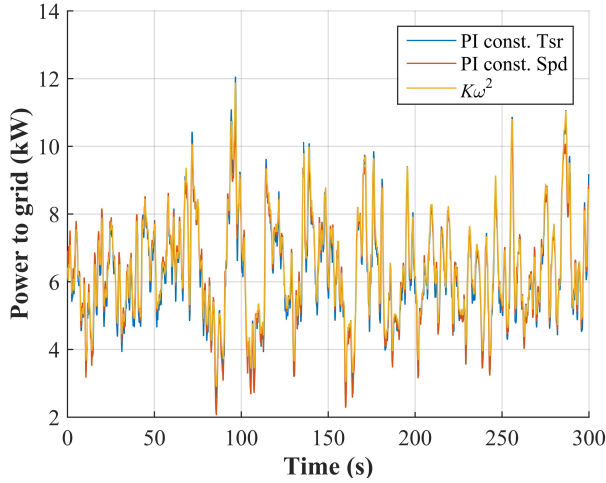


Fig. 9. Real power delivered to grid with 1 s moving average smoothing

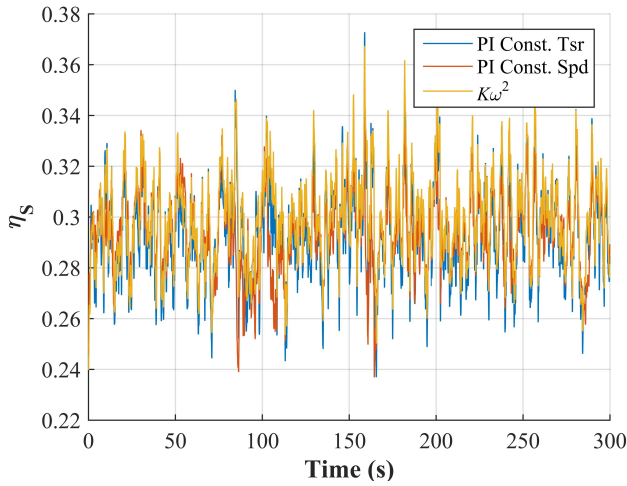


Fig. 10. Instantaneous system efficiency with 1 s moving average smoothing

variable, thus the turbine may only be reacting to fluctuations of 0.25 Hz or slower assuming an average velocity of 2.0 m/s across the rotor span. The presence and action of internal motor and generator control loops regulating speed and torque may also contribute to the difference.

E. Grid Integration Considerations

Real power demand for the town of Igiugig during August 1, 2014 (Fig. 12(a)) was analyzed to determine the implications of integrating a RivGen turbine into the grid. Demand exhibited a slow trend throughout the day, with mean power remaining stationary on the order of tens of minutes. During the day, there was a high load (neglecting outlying spikes) of 57 kW and a low of 26 kW. A 300 s portion of the time-series (Fig. 12(b)) at a power level near the low point of demand was selected to match the time scale of the emulated power output testing of the turbine. The demand in this time-frame remained relatively stable on the order of seconds between instantaneous

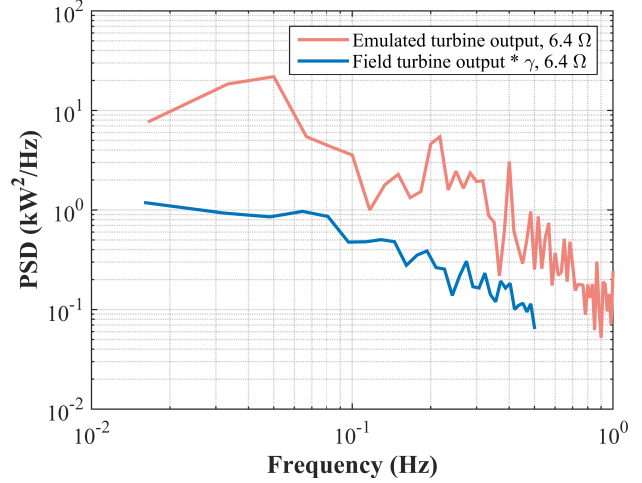


Fig. 11. Dynamic performance comparison between field-tested and emulated real power output

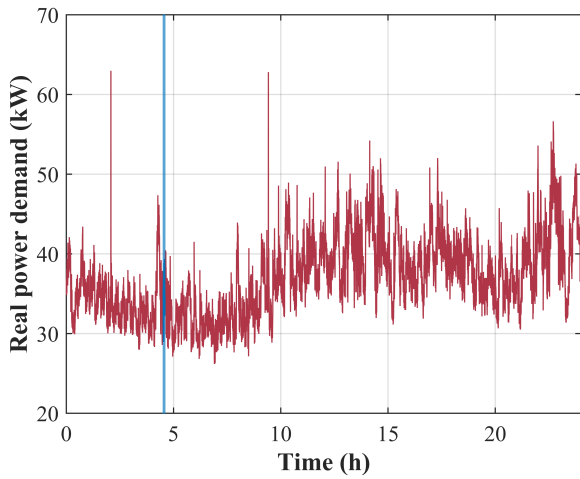
decreases and increases, as loads were switched off and on.

The turbine's emulated output scaled by $1/\gamma$ under a 6.4 Ω resistive load was compared to Igiugig's demand (Fig. 13) as if the demand profile of Fig. 12(b) occurred simultaneously with the input profile of Fig. 5. In these conditions a single RivGen turbine would not be able to meet the demand of the town, while two turbines could produce more power than needed at times. For the former case, an additional power source would be necessary for the demand to be met. For the latter case, a control strategy limiting power output or the ability to store energy produced in excess of demand would be needed.

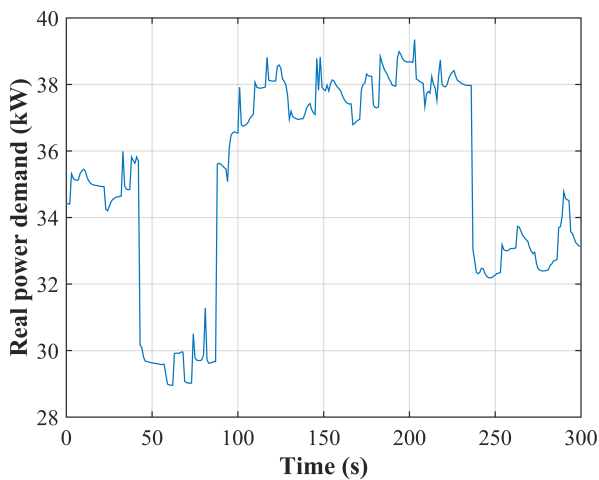
Power output from the turbine appears to change at a rate much faster than demand, as the inertia of the turbine is low, allowing it to react to short time-scale fluctuations in velocity. This is quantified by viewing the emulated power demand and turbine output in the frequency domain. These are compared with actual power output near optimal performance of the field-tested turbine on the same axes in Fig. 14. The turbine is expected to produce power more uniformly over a wider band of frequencies than would be required by the grid; the turbine's inertia is lower than the grid's, as evidenced by the steeper drop-off in frequency response. Therefore, should the turbine be incapable of meeting the full demand, a secondary source of power with a similar dynamic response would be needed to balance the high-frequency variability of the turbine output.

IV. DISCUSSION

High-resolution measurements of free-stream river velocity were used to seed synthetic turbulence generation software. Agreement between temporal flow statistics suggests the output of the program can be used as the resource input for simulation and emulation of a hydrokinetic turbine. One benefit of using such software is the ability to create a large number of representative time-series based on a limited number of field measurements. Parameters are randomly seeded in the



(a) Full day grid demand



(b) 300 s grid demand, shaded area in (a)

Fig. 12. Real power demand for Igiugig, 1 Hz sample rate, August 1, 2014

software such that unique time series with similar statistical characteristics can be created. Additionally, the software's output does not include contamination from sensor motion and Doppler noise, common concerns when utilizing acoustic techniques for flow characterization, but does not preserve all of the real flow information [13]. Finally, the software allows the creation of a spatially-gridded flow field, something difficult to obtain in the field.

Average electromechanical emulated power output is shown to agree with scaled field measurements of power output under similar inflow and loading conditions. Previous studies have compared results of emulation to hypothetical turbines and dynamic simulation [7], [12]. Emulation occurred at a lower power level than the actual turbine and with the inclusion of a virtual gearbox. Evaluation of the dynamic performance of the emulated turbine indicates a similarly trending, but higher variance response between 0.02 Hz and 0.5 Hz relative to that of the field turbine. The root cause of this difference will be investigated in future work.

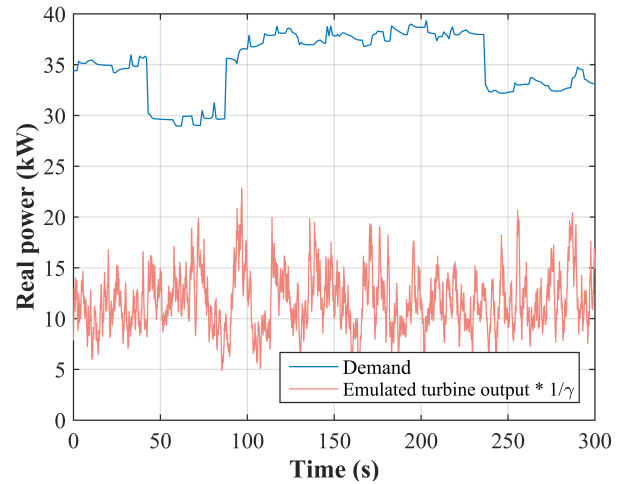


Fig. 13. Grid demand and emulated turbine output

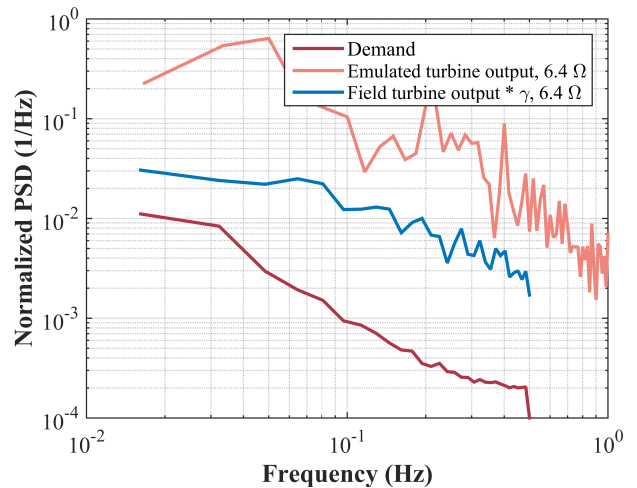


Fig. 14. Grid demand and emulated and field turbine output normalized PSD

The application of a virtual gearbox is the result of the high-torque/low-speed characteristics of the RivGen turbine being emulated on industry-standard electrical machines rated for low torque and high speed.

All evaluated turbine control strategies perform similarly in emulation given the input velocity time-series utilized for testing. This implies that, with a resource that is turbulent but whose mean does not vary substantially on the order of minutes, an aggressive controller tracking fluctuations in speed at a high frequency may not be necessary to achieve high average efficiency. This is evidenced by the strong performance of 'passive' control, where the loading was set to a static value that corresponded to an operating point near optimal for the mean flow speed. The results suggest a simple controller whose parameters vary on the order of minutes may be suitable. As these results are preliminary, future work will explore the role of control action update rate in obtaining desired performance.

The greatest benefits of the emulation technique are the ability to investigate various control strategies and the ability to evaluate actual power delivered to the grid in a laboratory environment. Determination of the viability of control techniques at low cost in the lab is preferred to exploratory testing during costly field operations. Results of this emulation testing will be used to inform control design for a future field trial of the RivGen turbine. However, if the actual turbine exhibits a similar dynamic response to control action as its response to turbulence, results described for controller performance during emulation may not directly translate to the physical system.

Comparison of the turbine's actual and emulated output with the demand of the community near where it may be deployed yields information on how grid integration may occur. The characteristics of a second generation source can be inferred based on the need to balance the turbine's variable output at high frequency under control with the strategies investigated. For example, if two turbine systems are utilized to meet the demand, one may need to employ a control strategy that tracks grid load, rather than maximizing power generation.

V. CONCLUSIONS

A representative resource model is taken as an input for laboratory emulation of a hydrokinetic turbine. A controllable motor is programmed to mimic the dynamics of the turbine as characterized in the field. Scaled power output during turbine emulation is in agreement with field trials under similar resource and resistive loading conditions, supporting the emulation technique. Nonlinear $K\omega^2$ and linear PI constant λ and ω control strategies are implemented in emulation. These controllers exhibit similarly efficient performance and maintain power output at near optimal values over a 300 s trial. The dynamic response of the emulated turbine is compared to the field turbine and is found to have a larger response to turbulent inflow, resulting in more variable instantaneous power output fluctuation. The turbine response is also compared to that of the grid of a small community near a potential turbine deployment site. The turbine's inertia is lower than the grid's, necessitating a secondary power source with a high-frequency response to meet power demand in the event the turbine's output cannot meet it alone. The electromechanical emulation technique is shown to be valuable for investigating control strategies and grid integration for a hydrokinetic turbine in a laboratory setting at a lower cost than field trials.

ACKNOWLEDGMENT

This work was supported in part by the US Department of Energy (DOE) EERE Postdoctoral Research Fellowship program and the DOE Marine and Hydrokinetic System Performance Advancement program. Use of the Conn emulator was provided by MaREI-Beaufort in Cork, Ireland. Special thanks are due to Judy Rea and Darren Mollaghan for their assistance with the rig and microgrid.

REFERENCES

- [1] S. Baral, S. Budhathoki, and H. Prasad Neopane, "Grid connection of micro hydropower, mini grid initiatives and rural electrification policy in nepal," in *Sustainable Energy Technologies (ICSET), IEEE Third International Conference on*, Kathmandu, Nepal, 2012.
- [2] D. Forbush and et al., "Performance characterization of a river current turbine in shear flow," (Forthcoming).
- [3] H. M. Kojabadi, L. Chang, and T. Boutot, "Development of a novel wind turbine simulator for wind energy conversion systems using an inverter-controlled induction motor," *Energy Conversion, IEEE Transactions on*, vol. 19, no. 3, pp. 547–552, 2004.
- [4] R. Alcorn and D. O'Sullivan, *Electrical Design for Ocean Wave and Tidal Energy Systems*. Stevenage: The Institution of Engineering and Technology, 2014.
- [5] S. Benelghali, M. E. H. Benbouzid, J. F. Charpentier, T. Ahmed-Ali, and I. Munteanu, "Experimental Validation of a Marine Current Turbine Simulator: Application to a Permanent Magnet Synchronous Generator-Based System Second-Order Sliding Mode Control," *IEEE Transactions on Industrial Electronics*, vol. 58, no. 1, pp. 118–126, 2011.
- [6] M. A. Vallet, S. Bacha, I. Munteanu, A. I. Bratcu, and D. Roye, "Management and Control of Operating Regimes of Cross-Flow Water Turbines," *IEEE Transactions on Industrial Electronics*, vol. 58, no. 5, pp. 1866–1876, May 2011. [Online]. Available: <http://ieeexplore.ieee.org/lpdocs/epic03/wrapper.htm?arnumber=5510139>
- [7] R. J. Cavagnaro, J. C. Neely, F. X. Fay, J. L. Mendia, and J. Rea, "Evaluation of electromechanical systems dynamically emulating a proposed hydrokinetic turbine," (In review).
- [8] M. Hauck, A. Rumeau, I. Munteanu, A. I. Bratcu, S. Bacha, D. Roye, and A. Hably, "A 1 : 1 prototype of power generation system based upon cross-flow water turbines," in *IEEE International Symposium on Industrial Electronics (ISIE)*, Hangzhou, 2012, pp. 1414–1418.
- [9] J. Rea, J. Kelly, R. Alcorn, and D. O'Sullivan, "Development and operation of a power take off rig for ocean energy research and testing," in *Proceedings from the 9th European Wave and Tidal Energy Conference*, Southampton, UK, 2011.
- [10] L. F. Kilcher, J. Thomson, and J. Colby, "Determining the spatial coherence of turbulence at mhk sites," in *Proceedings of the 2nd Marine Energy Technology Symposium, METS 2014, April 15-18*, Seattle, WA, 2014, pp. 1–7.
- [11] L. Kilcher, "Pyturbsim 0.4.2 documentation," <http://kilcher.github.io/pyTurbSim/>, 2015.
- [12] J. C. Neely, K. M. Ruehl, R. A. Jepsen, J. D. Roberts, S. F. Glover, F. E. White, and M. L. Horry, "Electromechanical emulation of hydrokinetic generators for renewable energy research," in *IEEE Oceans, September 23-27*, San Diego, CA, 2013, pp. 1–8.
- [13] J. B. Richard, J. Thomson, B. Polagye, and J. Bard, "Method for identification of doppler noise levels in turbulent flow measurements dedicated to tidal energy," *International Journal of Marine Energy*, vol. 3, no. 4, pp. 52–64, 2013.